Localized ac response and stochastic amplification in a labyrinthine magnetic domain structure in a yttrium iron garnet film

M. P. DeFeo and M. Marchevsky
Physics Department, Syracuse University, Syracuse, New York 13244, USA
(Received 3 February 2006; revised manuscript received 11 April 2006; published 9 May 2006)

Local ac dynamics of the labyrinthine magnetic domain phase in a yttrium iron garnet was studied with scanning Hall microscopy. The harmonic response of the domain walls in the course of the field-driven labyrinth-to-stripe transition is found to be strongly localized at the disclination defects of the labyrinthine structure. The amplitude of the domain wall oscillations in the vicinity of disclination defects is amplified when Gaussian white noise is added to the harmonic drive. Possible microscopic origins of the noise-induced enhancement of the ac response are discussed.

DOI: 10.1103/PhysRevB.73.184409 PACS number(s): 75.70.Kw, 75.70.Ak, 05.40.−a, 85.30.Fg

I. INTRODUCTION

Unidirectional modulated phases are ubiquitous in condensed matter physics. A broad range of systems, including liquid crystals,[1] type-I superconductors,[2] diblock copolymers,[3] ferromagnetic films, and many others exhibit lamellar spatial modulation and common types of topological defects. While structural and dynamic transitions of the lamellar-modulated systems have been extensively studied, there are still unanswered questions regarding thermodynamic stability and microscopic-scale dynamics. The complexity is often related to the metastable nature of the lamellar phases and the special role of topological constraints in their structural evolution. One of the well-known systems exhibiting lamellar modulation is the labyrinthine magnetic domain structure found in ferromagnetic films with perpendicular anisotropy, such as yttrium iron garnets.[4] In garnets, the labyrinthine phase is formed due to the nucleation and the bifurcation of the minority domain component as an external magnetic field is lowered from saturation. During the demagnetization process, domains branch and form loops resulting in an array of oppositely-charged $+1/2$ and $-1/2$ disclinations in the majority domain component.[5] The pattern evolution is reminiscent of the disclination-unbinding mechanism characteristic of the Kosterlitz-Thouless phase transition and involves a long-range dipolar pair interaction between defects.[6] However, as the domains cannot cross or reconnect, the disclination arrays move collectively and do not equilibrate completely resulting in a metastable configuration.[7] An additional impeding factor in energy minimization is domain wall pinning at point defects. A combination of topological constraints and point pinning causes magnetic nonlinearity, coercivity, and hysteresis in ferromagnetic materials.

Even more rich and complex are the dynamics of the domain structures. Threshold phenomena in these systems were first seen nearly a century ago[8] and studied in greater detail recently, both theoretically[9] and using real-space imaging.[10] As was recently shown, domain wall dynamics can be influenced by random noise,[11] due to the occurrence of the stochastic resonance (SR). The latter was originally proposed[12] as a mechanism of climate change and later adopted for a great variety of physical systems.[13] Random noise causes the dynamic height variation of adjacent potential wells resulting in the successive hopping of the system between its potential minima. When a periodic drive is added, a stochastic synchronization takes place when the average time between two consecutive noise-induced transitions is roughly equal to the half-period of the periodic force.[14] The effect is observed as a peak in the systems periodic response at a nonzero amplitude of the noise. Earlier, SR in domain systems was observed for a straight segment of the domain wall which is constrained between two microscopic pinning sites and changes its curvature when driven externally.[11,15–18] However, point pinning is not the only source of multistability in domain systems. Long-range coupling of the disclination defects and topological constraints in the pattern favor a rich scope of self-organizational dynamics and can potentially contribute as well to the SR phenomenon. Understanding the noise-driven magnetic states is important for various technological applications including novel field sensors and magnetic memory technologies.

II. EXPERIMENT

In this paper, we study the local ac motion of the domain walls in the labyrinthine domain structure of yttrium iron garnet. We observe the localization of the ac magnetic response at the disclination points in the domain pattern and demonstrate the stochastic amplification of this response upon application of magnetic white noise. The sample is a film of yttrium iron garnet (Ca, Ge substituted), 5 μm in thickness, epitaxially grown on a translucent gadolinium gallium garnet substrate. The saturation magnetic field is approximately 75 G with the easy axis of magnetization perpendicular to the surface. The room-temperature coercivity field is <0.1 G. Scanning Hall microscopy was used to study the structure and dynamics of the magnetic domains. The Hall probe, fabricated from a 2DEG GaAs-AlGaAs heterostructure, has an active area of 1.5 μm^2 and a typical room-temperature dc sensitivity of ~ 1 G, which is ~ 100 times smaller than the local field variation created by the magnetic domains at the sample surface. The probe is scanned over an area of 35×35 μm with a piezoelectric scanner. A solenoid is placed around the apparatus in order to apply a homoge-

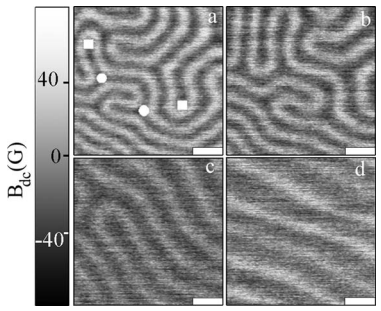

FIG. 1. Evolution of the laminar state of the domain pattern from the disordered labyrinth state as dc field increases. (a) Domains in the labyrinth state in the absence of a dc field and small (1.7 G) ac field, which is constant through the sequence. Squares and circles mark oppositely charged disclinations. (b) When the dc field is increased to 24 G, the minority domain component reduces in width while the majority domain component expands. Some disclination pairs annihilate reducing the overall defect density. (c) As the dc field is increased to 35 G, a drastic structural change takes place, as nearly all disclination pairs annihilate, thus reducing the accumulated strain. (d) When the dc field approaches 44 G, the domain system switches over to the laminar state; all topological defects have now been annihilated. Scale bars in the images are 10 μm.

neous bias field along the easy magnetization axis of the sample.

The labyrinthine domain state was prepared by ramping up the external field B_{dc} from 0 to 81 G to first saturate the sample, and then subsequently reducing it back to zero over a 2 s time period to induce domain nucleation. The subsequently prepared labyrinthine domain configurations show a reproducible equilibrium domain period and the density of the topological defects but no significant cross-correlation in real space, suggesting an absence of strong pinning sites in the sample. Once the labyrinthine pattern is formed in the demagnetized state, a constant dc field is reapplied in the same direction as initially. As the sample is being remagnetized, the width of the domains aligned with the external field increases, while the width of domains in the opposite orientation decreases. The global topology of the domain pattern during this process is unchanged until a certain threshold field is reached. At the threshold value, the structure switches abruptly to a different, less defective configuration, thus reducing the magnetic strain and minimizing the global free energy of the system. Eventually, at higher fields, the number of the topological defects in the domain system decreases and the system crosses over to a laminar, stripe state. This evolution has much in common with the disclination-unbinding mechanism typical for liquid crystals[1] and has been studied earlier,[6,19] analyzed theoretically,[20] and seen in simulations.[21,22] The labyrinth-to-stripe phase transition is hysteretic but it is reversible and the topological defect concentration may be fairly well controlled with the applied magnetic field. In Fig. 1, imaging data for the typical stages of the labyrinthine pattern transformation are shown. We found that within the imaged area, the motion of the disclinations (branching points and end points of the pattern) occurs in a discontinuous way. An initial field increase would typically preserve the structure, causing the relative width of the opposite domains to change. However, as the critical magnitude of the magnetic strain is achieved at a certain applied threshold field B_{th}, the pattern switches to a lower energy configuration and some disclinations annihilate. The threshold field B_{th} was found to be in the range of 25–40 G, dependent upon the initial "defectiveness" of the labyrinthine domain configuration.

We study the local response of the domain system to a small (2–8 G) harmonic magnetic field applied along the easy axis of magnetization using a small 40 turn modulation coil placed directly underneath the sample. Our ac measurement technique is based upon a local detection of the time-varying magnetic field. When the Hall probe is positioned above an oscillating domain wall, the displacement of the wall produces a proportional Hall signal at the frequency of the drive. The amplitude and phase of the local ac Hall signal were acquired simultaneously using an SR850 lock-in amplifier and mapped spatially by scanning the sensor at a distance of $\sim$0.1 μm above the sample surface. Given the typical ac sensitivity of the Hall sensor of about 0.1 G in the frequency range 10–1000 Hz, linear dimensions of the sensor of $\sim$1.5 μm and domain stray field variation of $\sim$100 G, the minimal detectable amplitude of the periodic domain wall displacements is $\sim$0.1 nm. In practice, however, the sensitivity is limited by other factors, such as the thermal drift of the piezoscanner. In our experiments, amplitudes of $\sim$100 nm were typically registered, which is still only a small fraction of the domain pattern period ($\sim$5 μm), therefore our ac measurements did not introduce any significant perturbations to the local magnetic energy landscape. We find that the domain wall response (with the background driving signal subtracted) is below a detectable level for ac field amplitudes less than 7.3 G. At larger amplitudes, the wall susceptibility increases linearly with the applied ac field. Also, the localization of the strongest ac response near the end points of the domain pattern is seen. The localization becomes much more pronounced when a near-threshold dc bias field $B=38$ G is applied in addition to the ac excitation. In Fig. 2(a), the dc, ac, and phase images of the same area of the sample taken simultaneously are shown. We observe peculiar domain wall oscillations in the vicinity of the end-points of the domain pattern, primarily at the "loops" in the opposite domain component surrounding the end points. These loops appear to be the most susceptible parts of the pattern. In some experiments the surrounding loops oscillate as well. These oscillations are observed as characteristic "ripples" appearing between the nearby end points in the pattern. Similar images with the loop oscillations localized within a narrow line connecting end points separated by 7–10 domain periods were observed in earlier experiments where an in-plane gradient of the ac field ($\sim$30% across the sample of $\sim$3 mm width) was present.[23] As our measurements correspond to an intermediate stage of the labyrinth-to-stripe transition, the enhanced ac response of the disclination points suggests their greater mobility, which is in concert with the two-dimensional (2D) disclination unbinding mechanism.[6] The latter implies the evolution of the domain pattern via motion and subsequent annihilation of the oppositely-charged disclination defects. The phase images of

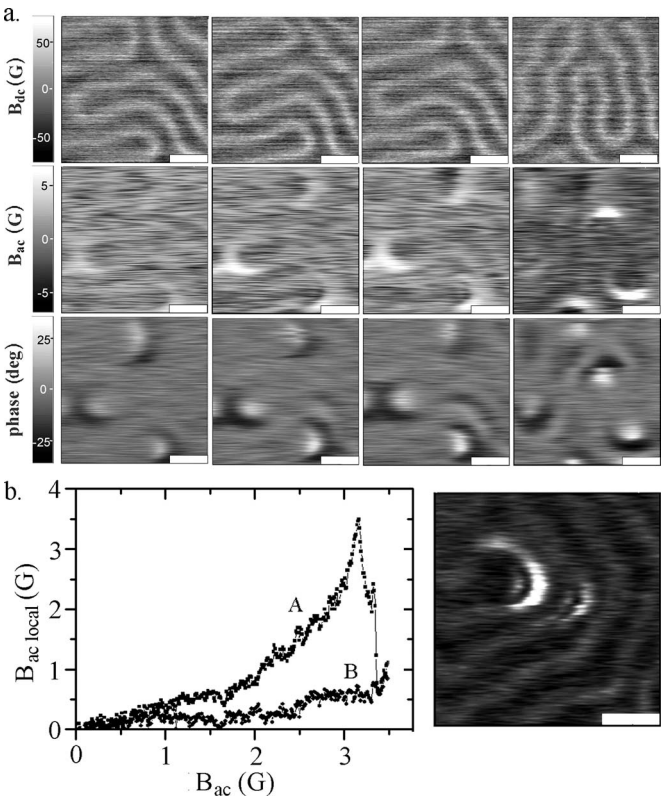

FIG. 2. (a) dc, ac and phase images taken simultaneously at B_{dc}=60 G and B_{ac}=1.4, 1.92, 2.4, and 2.88 G, respectively, from left to right. Loops in the domain pattern appear as regions of the largest ac response and a significant phase shift. The abrupt change of the pattern occurs at B_{ac}=2.88 G. (b) Left: Local harmonic ac response of a domain loop taken at a distance of ~0.1 μm from the sample. Measurements were taken in the presence of B_{dc}=60 G. The jump at B_{ac}=3.2 G occurs as a result of the domain depinning. Right: ac image of a similar domain loop, oscillating under an ac field of 3.5 G in the presence of a B_{dc}=37.8 G. The ac amplitude scale is ~14 G (black to white). Scale bars in the images are 10 μm.

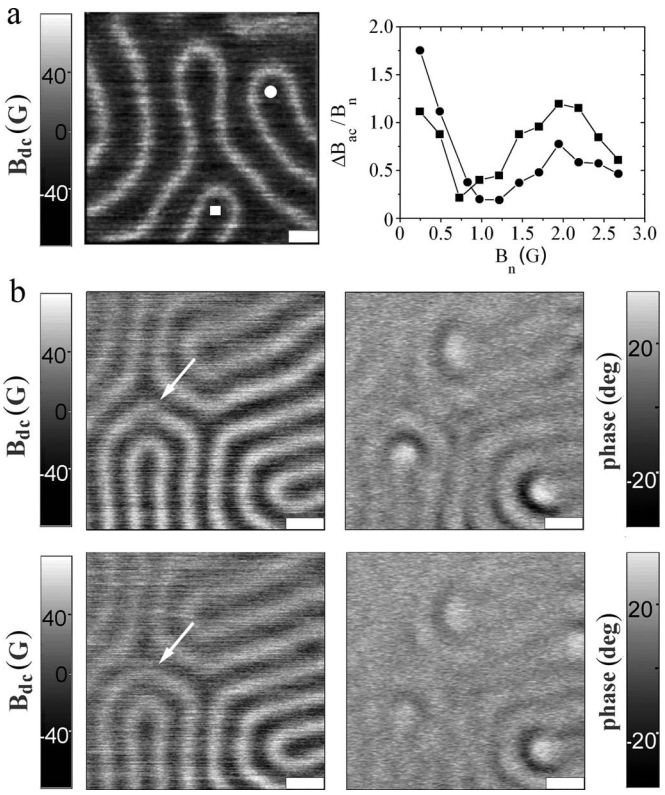

FIG. 3. (a) Left: dc image of the domain structure at applied B_{dc}=37.8 G and B_{ac}=2.9 G (f_{ac}=777 Hz). Two "loops" are present in proximity to each other. Right: the corresponding plots of the local ac signal increase due to noise, ΔB_l (see text) measured at the positions of the two loops (one is marked with the square and another with the circle) at the same B_{dc} and B_{ac} applied. The noise field was ramped from 0 to 2.68 G. For both loops the $\Delta B_l/B_n$ peaks at a nonzero amplitude of the magnetic noise. (b) Dc (left) and phase (right) images taken at B_{ac}=3 G in the presence of B_{dc} =38 G bias field and two different noise field amplitudes B_n =1.7 G (top) and B_n=0.73 G (bottom). Phase shift of up to 30 deg is seen near the disclination point. Formation of a kink in the curved domain (shown in dc images with arrows) is observed as the noise amplitude is increased. Scale bars in the images are 5 μm.

the disclination points are even more striking: they show up as areas of the ac phase shift of 20°–30°, also indicative for a strong nonlinearity of the local response [see Fig. 2(b)]. Pinning-dependent phase lags of the local ac susceptibility for the driven domain walls were recently predicted theoretically.[24] In contrast to the zero dc bias results, the ac amplitude response of the disclination points in our experiment is strongly nonlinear. In Fig. 2(b) (left), the plot of the local $B_{ac\ local}$ (with background ac signal B_{ac} subtracted) measured near the endpoint of another labyrinthine structure is shown. We found that phase images clearly "map" the end point positions in the pattern even at the smallest (<0.5 G) ac amplitudes applied. While the local ac susceptibility of the disclination regions is dependent on the magnitude of the dc bias field, we find it to be independent of the ac frequency in the range of 77 Hz–3.5 kHz.

Next, Gaussian white noise is applied in addition to driving the ac harmonic field B_{ac}=0.8 G (3.1 kHz) and dc bias field B_{dc}=38 G. The noise waveform is generated with Labview software and applied using the same modulation coil driven by an ac current calibrator (Valhalla Scientific 2500). The calibrator-based magnetic modulation setup has a linear frequency response in the 0–10 kHz frequency range. We simultaneously acquired dc images of the domain pattern and ac amplitude images of the local domain response as noise was ramped down from the maximal value B_n=2.68 G (mean Gaussian value) to zero, with a 0.24 G step between the consecutive images. Again, a strong local ac response is seen around the end points of the domain pattern. Figure 3(a) (left) shows the dc domain pattern containing two strongly responding domain loops separated by ~20 μm distance. The ac images corresponding to this area were cropped to 2.5×6 μm around the "loops" and treated with a median filter, to reduce accidental noise spikes. The average values of the local ac signal increase due to noise, $\Delta B_l=(B_l-B_{l_0})$, are obtained from the cropped images and the ratio $\Delta B_l/B_n$ is plotted in Fig. 3(a) (right) as a function of the noise intensity B_n;here B_{l_0} is the local ac signal in the absence of noise. Both

curves reach their maxima at roughly the same noise intensity of 2 G (mean Gaussian value) although the local signal amplitudes ($B_{ac\ local} - B_{ac}$) at which the maximum occurs are different. We repeated the experiment for various configurations of the labyrinthine structure in several independent experimental runs and similar results were obtained.

III. DISCUSSION

In Fig. 3(b), dc and phase images of a different area of the sample are shown. The dc bias field is 38 G, the ac harmonic field is 3 G, and the noise amplitudes are 0.73 G (bottom) and 1.7 G (top), respectively. We observe phase shifts of the local ac signal of up to 30 deg comparable to the results in Fig. 2 where no noise was applied. Measurements were also taken at the different ac driving frequencies ranging from 250 Hz to 3.1 kHz and the data showed no noticeable frequency dependence of the $\Delta B_l / B_n$ peak position. Interestingly, the same frequency independence of the signal-to-noise ratio (SNR) was earlier seen[11] for an oscillating domain wall segment and interpreted as a stochastic resonance. In fact, the classic SR scenario assumes both frequency and noise amplitude dependence of the SNR.[13] We would therefore deem our observations as SR with caution. Babcock *et al.*[25] report that the ac field has no significant influence on the domain motion for frequencies above 200 Hz, which is surprising given the typical flexural resonances of the domain walls are in a 10–100 MHz range.[26] On the other hand, the Kramers rate for a pinned domain segment in a similar material was estimated to be within 10^{-4}–20 Hz.[15] One can speculate that topological constraints impede the system response at higher frequencies and the characteristic Kramers rate is specific for the particular local domain configuration. Alternatively, the frequency-independent position of the $\Delta B_l / B_n$ peak in our experiments may be attributed to the "thresholding effect".[27] Further investigation of the ac frequency dependence is needed.

Stochastic amplification is usually indicative of multistability and threshold type dynamics.[28] In the domain system, one obvious cause of multistability is the local potential landscape created by pinning centers in the crystalline lattice. When the system is brought above threshold and driven with an ac field, the domain wall switches between two of the many possible configurations defined by the individual pinning centers. Pinned domain wall segments can "buckle" and change their curvature abruptly.[11] When depinned, domain walls jump towards the next potential minima.[29] We applied short pulses of magnetic field to our sample, in addition to the near-threshold constant B_{dc}, and followed the patterns evolution. Often, the overall topology would not change after subsequent pulses, but numerous small structural deviations of 0.5–3 μm, mainly near the "end points" will appear. Random pinning sites stabilize similar domain states and local deviations between these states are a measure of the characteristic distance between those sites. Other studies[30] report pinning a site concentration of $\sim 10^{10}$ cm^{-3} for epitaxially grown garnets. The latter number translates into $\sim$2–3 μm distance between the neighboring pinning sites, in concert with our pulsed sequence data. However, point pinning induced constraints coexist with a configurational bistability that is intrinsic to the labyrinthine configuration. Although disordered globally, the labyrinthine state is characterized by a short-range order. Magnetic domains form distinct areas (plaquettes) of unidirectional modulation[31] as a result of free energy minimization. These ordered areas are polygonal in shape and are enveloped by tilt boundaries whose terminal points are disclinations or dislocations. Segments forming the plaquettes statistically adhere to a preferred segment length ξ and angle of intersection with the tilt boundary $\pm\alpha$. These parameters are a function of domain period which is intrinsic to the system.[31,32] The preferred kink angle for our system at $B=0$ is $\alpha \simeq 53°$ [Fig. 4(a)]. Close to the disclination end point, the curvature of the domains is large but continuous, without kinking. The application of the noisy oscillating external field appears to repetitively straighten the domains and "kink" the structure. This phenomenon is illustrated in Fig. 4(b), where the two magnified portions of the dc images from Fig. 3(b) are shown. The increase of the noise field (image on the right) leads to the appearance of the kink in the previously uniformly curved loop. One can propose that looped and kinked configurations constitute the two nearest minimal energy configurations between which the domain wall oscillates. Topological bistability and pinning centers cause potential landscape variations of the same characteristic length scale. Hence the combination of the point pinning and the intrinsic topological constraints causes stochastic ac amplification around the end points.

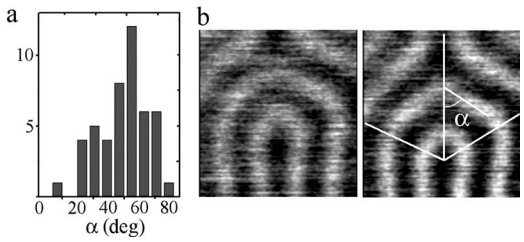

FIG. 4. (a) Histogram displaying the probability distribution for a system of magnetic domains to kink at a certain angle measured in degrees. Data are acquired from two different domain configurations with applied $H_{dc}=10.8$ G. (b) Magnified portions of the domain loops shown with arrows in Fig. 3(b) and corresponding to the different applied noise amplitudes, $B_n=0.73$ G (left) and $B_n=1.7$ G (right). Amplitude scale was adjusted to improve contrast. Clear evolution from the uniformly curved to the "kinked" local configuration is seen as the noise amplitude is increased. The tilt boundaries are shown in the right figure with white lines.

IV. SUMMARY

We studied the local ac response of magnetic domains in the labyrinthine phase in the yttrium iron garnet film. The localization of the driven oscillatory motion occurs in the vicinity of the disclination defects of the labyrinthine structure. When driven with a random noise magnetic field, stochastic amplification of the defect-centered oscillatory motion is observed. Our results are relevant to a great number of

disordered systems with threshold dynamics. The nonequilibrated labyrinthine domain structure is an example of a two-dimensional glass[7,32] and the observed defect-centered local ac response may thus be characteristic for other glassy systems. Ferromagnetic thin films may be coupled to other systems, such as superconductors where domain-induced superconductivity has been recently reported[33] and our results suggest different ways of local modulation of the vortex state. The observed stochastic ac amplification can be of relevance for development and sensitivity improvement of the garnet-based field sensors and transducers.

ACKNOWLEDGMENTS

The authors are grateful to S. Bhattacharya and M. J. Higgins (NEC, Princeton) for providing essential equipment support and the garnet sample and to the Syracuse University for funding this work.

[1] P. G. de Gennes and J. Prost, *The Physics of Liquid Crystals* (Clarendon, Oxford, 1993).
[2] T. F. Faber, Proc. R. Soc. London, Ser. A **248**, 460 (1958).
[3] C. Harrison, D. H. Adamson, Z. Cheng, J. M. Sebastian, S. Sethuraman, D. A. Huse, R. A. Register, and P. M. Chaikin, Science **290**, 1558 (2000).
[4] A. P. Malozemoff and J. C. Slonczewski, *Magnetic Domain Walls in Bubble Materials* (Academic, New York, 1979).
[5] J. Toner and D. R. Nelson, Phys. Rev. B **23**, 316 (1981).
[6] M. Seul and R. Wolfe, Phys. Rev. Lett. **68**, 2460 (1992).
[7] B. Reimann, R. Richter, and I. Rehberg, Phys. Rev. E **65**, 031504 (2002).
[8] H. Barkhausen, Phys. Z. **20**, 401 (1919).
[9] S. Zapperi, P. Cizeau, G. Durin, and H. E. Stanley, Phys. Rev. B **58**, 6353 (1998).
[10] D.-H. Kim, S.-B. Choe, and S.-C. Shin, Phys. Rev. Lett. **90**, 087203 (2003).
[11] A. N. Grigorenko, P. I. Nikitin, and G. V. Roshchepkin, JETP Lett. **65**, 828 (1997).
[12] R. Benzi, A. Sutera, and A. Vulpiani, J. Phys. A **14**, 453 (1981).
[13] L. Gammaitoni, P. Hanggi, P. Jung, and F. Marchesoni, Rev. Mod. Phys. **70**, 223 (1998).
[14] H. A. Kramers, Physica (Utrecht) **7**, 284 (1940).
[15] A. N. Grigorenko, P. I. Nikitin, A. N. Slavin, and P. Y. Zhou, J. Appl. Phys. **76**, 6335 (1994).
[16] P. Ruszczynski, L. Schimansky-Geier, and I. Dikshtein, Eur. Phys. J. B **14**, 569 (2000).
[17] I. Dikshtein, A. Neiman, and L. Schimansky-Geier, J. Magn. Magn. Mater. **188**, 301 (1998).
[18] S. W. Sides, R. A. Ramos, P. A. Rikvold, and M. A. Novotny, J. Appl. Phys. **81**, 4497 (1997).
[19] P. Molho, J. L. Porteseil, Y. Souche, J. Gouzerh, and J. C. S. Levy, J. Appl. Phys. **61**, 4188 (1987).
[20] D. Sornette, J. Phys. (Paris) **48**, 151 (1987).
[21] J. R. Iglesias, S. Gonçalves, O. A. Nagel, and M. Kiwi, Phys. Rev. B **65**, 064447 (2002).
[22] A. D. Stoycheva and S. J. Singer, Phys. Rev. Lett. **84**, 4657 (2000).
[23] M. Marchevsky (unpublished).
[24] H.-T. Wang and S. T. Chui, Phys. Rev. B **60**, 12219 (1999).
[25] K. L. Babcock and R. M. Westervelt, Phys. Rev. A **40**, 2022 (1989).
[26] B. E. Argyle, W. Jantz, and J. C. Slonczewski, J. Appl. Phys. **54**, 3370 (1983).
[27] L. Gammaitoni, Phys. Rev. E **52**, 4691 (1995).
[28] L. Gammaitoni, F. Marchesoni, E. Menichella-Saetta, and S. Santucci, Phys. Rev. Lett. **62**, 349 (1989).
[29] K. S. Novoselov, A. K. Geim, S. V. Dubonos, E. W. Hill, and I. V. Grigorieva, Nature (London) **426**, 812 (2003).
[30] G. Vértesy, I. Tomás, and Z. Vértesy, J. Phys. D **35**, 625 (2002).
[31] M. Seul, L. R. Monar, L. O'Gorman, and R. Wolfe, Science **254**, 1616 (1991).
[32] M. Seul, L. R. Monar, and L. O'Gorman, Philos. Mag. B **66**, 471 (1992).
[33] Z. R. Yang, M. Lange, A. Volodin, R. Szymczak, and V. V. Moshchalkov, Nat. Mater. **3**, 793 (2004).